FATIGUE ANALYSIS OF A MEDIUM STRENGTH Al-Mg ALLOY 5083

J.D. COSTA*, C.M. BRANCO** and J.C. RADON***

The paper reports the results of a fatigue crack propagation study on the Al-Mg 5083-O. da/dN, ΔK data was obtained in tension and bending for three different stress ratio values. The fatigue crack propagation of both straight and semi-elliptical cracks was analysed. For that purpose crack aspect ratio data was generated and a good correlation was obtained against available theoretical solutions in the literature.

Crack closure data was obtained and used to calculate effective values of ΔK. Fatigue crack growth rate when plotted as a function of ΔK_{ef} has shown not to be dependent of stress ratio. For $R>0.8$ the amount of crack closure at the crack tip is negligible. Short crack growth data was obtained in square section specimens with a sharp notch.

INTRODUCTION

The medium strength aluminium alloy 5083-O is largely used as a structural material due to its excelent weldability and strength. The fracture toughness behaviour at low temperatures is ductile with no temperature transition as shown in previous work carried out by Costa and Branco (1), where COD and J results were obtained in the temperature range -200^0 to $+150^0$C. Fatigue data is however comparatively scarce in comparison with 2000 and 7000 series aluminium alloys. Hence the main objective of this research program is to characterize the fatigue behaviour of a 5083 aluminium alloy, both for long crack and short crack propagation.

In previous work by the authors (2) fatigue crack propagation results were obtained in CT and CCT specimens. The CCT specimens were provided with a central semi-elliptical notch. The influence of stress ratio (R=0; 0.5 and 0.8) and crack shape (full depth and semi-elliptical) was assessed. Crack closure data were obtained for three values of stress ratio. The crack closure parameter U initially proposed by Elber (3) was used to obtain the effective values of ΔK, ΔK_{ef}. The crack velocity da/dN when plotted versus ΔK_{ef} gave a very good correlation indepen

*SAEM, University of Coimbra, 3000 COIMBRA - PORTUGAL
**CEMUL, Lisbon Institute of Technology, 1096 LISBON CODEX - PORTUGAL
***Imperial College, London SW7 - UNITED KINGDOM

dent of stress ratio.

For short cracks there is evidence in the literature by Ritchie (4), Miller (5,6), that for the same ΔK level crack growth rate is higher than for long cracks.

In Ritchie's work (4), comparison of results obtained in specimens with micro--corner cracks against long crack data obtained in CT and CCT specimens confirm this trend. The absence of crack closure in short cracks seems to be the main cause to explain the higher crack growth rates in very short cracks. However there is insuficient data to demonstrate this conclusion specially when short crack growth from tiny notches at specimen surface is concerned.

In this paper fatigue crack propagation data is presented for aluminium alloy 5083-0, both for short cracks and long cracks. The parameters analysed were stress ratio, loading mode (tension and bending) and crack aspect ratio. Crack closure measurements were also taken and the results were used in the fatigue predictions.

EXPERIMENTAL

Costa (7) has obtained the chemical composition and mechanical properties of of the Al-Mg alloy 5083-0 and these are: 4.5%M_g; 0.55%M_n; 0.37%F_e; 0.5%N_i; 0.12%C_u; 0.1%Z_n; 0.05%S_n; 0.05%T_i.

Longitudinal direction of the plate material: σ_{UTS}=320.8MPa; σ_{ys}=180MPa; ε_f=18.2%.

Cyclic stress-strain curve; $\frac{\Delta\varepsilon_p}{2} = 0.273\ (2N_r)^{-0.664}$

Fatigue crack propagation was obtained in CT, CCT specimens and square bars. The specimen thickness was 12mm and the loading modes were tension and bending. The tension tests were carried out in a load-controlled servohydraulic machine. The load wave was constant amplitude sinusoidal with a frequency varying from 20 to 50Hz. The bending tests were performed in a fatigue testing rig specially built for that purpose. The frequency used in the bending tests was 25Hz.

For both bending and tension tests three different stress ratio values were applied (R=0.05; R=0.5 and R=0.8). The short crack specimens were provided with a micro corner notch with approximately 50μm long in both directions. This micro--notch was obtained by pressing a razor blade against the specimen surface with a controlled force of 100gr. The micro-notch dimensions were checked in all the specimens before the fatigue tests.

Crack length measurement in the long crack specimens was made with an AC potential drop system in the depth a direction and a travelling microscope in the c direction (crack length). The short crack measurements were made in a metallographic microscope with 1000x magnification. For that purpose the specimen was taken during the test from the fatigue machine at periodic intervals, polished and etched, and finally observed at the microscope. With this technique it was possible to detect cracks short as 20μm long from the notch root. The readings were made at both directions of the corner crack.

Crack closure measurements (opening loads) were obtained with a micro Elber type gauge placed near the crack tip with the measuring points above and below the crack surfaces. The plots load against crack opening were obtained and from these the opening loads were obtained for different ΔK values.

For the CT and CCT specimens the da/dN; ΔK plots were obtained with the five points polynomial method defined in the ASTM specification (8). The tangent method (8) was chosen for the square specimens with micro-corner cracks.

RESULTS AND DISCUSSION

Crack shape results are presented in Figures 1 and 2. The curves refer to the plots of a/c against the normalised crack depth a/B both for short corner cracks and semi-elliptical cracks in tension and bending. The short corner crack data is only for a/B <0.1. Some scatter was obtained in the a/c results in short cracks. This is due to the fact that crack initiation took place in most cases in one direction only (a or c) causing therefore delay in the other direction. However, as the crack grows and a/B increases crack propagation tends to equalize in both directions and the scatter is reduced near a/c=1 for higher values of a/B. In the range a/B values presented, no influence was observed of stress ratio and loading mode.

The influence of loading mode (bending or tension) can be seen in Figure 2 for the long cracks. In bending the crack aspect ratio increases from a/c=0.3 to a/c=0.6 for a/B=0.3 and afterwards decreases markedly. In tension there is a considerable increase of a/c till 0.9 for R=0 and 0.8 for R=0.5. After 0.8 there is a slight reduction in the a/c values. This behaviour shows that in tension the cracks tend to stabilize in the semi-circular shape while in bending the trend is towards the semi-elliptical shape. The influence of stress ratio in the crack shape is therefore different for bending and tension without any visible explanation.

In the micro corner cracks ΔK was computed with the Pickard polynomial equations (9). The theoretical curves in Figure 2 were obtained with the Raju and Newman equation (10). Also the ΔK values for the semi-elliptical cracks were calculated with this equation. The agreement between the experimental crack aspect ratio values and the theoretical predictions in Figure 2 is good.

In Figure 3 a typical plot da/dN and dc/dN against $\underline{a}$ and $\underline{c}$ is shown for the corner short cracks with size below 1000 μm. It is seen that crack growth rate increases with crack length till crack depths near 100 μm. Between 100 and 300 μm crack growth rate decreases and afterwards the growth rate is approximately constant. Crack closure may explain this behaviour since the crack surfaces are open for cracks less than 100 μm long and closure increases gradually for sizes between 100 and 300 μm tending towards a stable value for crack depths above 300 μm a typical size for the begining of the long crack regime.

The U factor is plotted against ΔK in Figure 4 including the results for the CT and CCT specimens. For the CT specimens the results in curve 1 of Figure 4 show that crack closure is very important specially for R=0. For this stress ratio value, U is less than 0.75 for ΔK < 5MPa$\sqrt{m}$ and reaches 0.35. For ΔK > 7MPa$\sqrt{m}$ U is independent of ΔK (U=0.75). For R=0.5 the values of U are above those of for R=0. Crack closure is only observed for $\Delta K < 5MPa\sqrt{m}$ ($U \simeq 1$ for $\Delta K > 5MPa\sqrt{m}$). For R=0.8 crack closure was not observed and therefore U=1 for all ΔK values tested. In the CCT specimens and for R=0 the U values are lower than those in the CT specimens and U does not remain constant as in the CCT specimens.

Figure 5 shows da/dN plotted against ΔK_{ef} in the CT specimens and for the three values of R. ΔK_{ef} was calculated from the U values plotted in Figure 4. A good correlation was obtained between da/dN and ΔK_{ef} without any dependence of stress ratio. Hence in this alloy the mean stress effect on crack propagation is mainly due to crack closure.

Region II of crack propagation shows two slopes in the da/dN; ΔK diagram. This is often found in other aluminium alloys and FCC metals as reported by Yoder et al (11), Pusch (12) and is explained by the relation Costa (13) between the dimension of the cyclic plastic zone in plane strain and certain microstructural parameters such as subgrain size, grain size and dispersoid spacing who create three transition points in the da/dN; ΔK curve.

The da/dN; ΔK results for the micro-corner cracks are plotted in Figure 6 together with the long cracks data in CT and CCT specimens and for the three stress ratio values. For micro-cracks with sizes below 300 μm the crack growth rate is higher than for the long cracks (CT and CCT specimens). Also fatigue crack propagation still takes place for ΔK values below the threshold level ΔK_{th} for long cracks (e.g. $\Delta K_{th} = 3.3MPa\sqrt{m}$ for R=0 and $\Delta K_{th} = 2MPa\sqrt{m}$ for R=0.5). For cracks greater than 300 μm there is a good agreement between the results in the CT and CCT specimens. The long cracks curve for R=0.8 where crack closure is insignificant fits very well with the experimental data in short cracks thus confirming the fact that crack closure is virtually absent in microcracks. Note that as crack closure is increasing with crack length the curves da/dN; ΔK for specimens with long cracks join with the corner crack data when the crack length is above 300 μm (Figure 6).

CONCLUSIONS

1. Good correlation was obtained both in bending and in tension between the experimental results of crack aspect ratio (a/c versus a/B) and the theoretical predictions.

2. Both for through and semi-elliptical cracks fatigue crack growth rate does not depend on stress ratio when correlated against ΔK_{ef} for crack closure.

3. For micro-cracks with size below 300 μm and for stress ratio values of R=0 and 0.5 fatigue crack propagation occurs for ΔK values below the threshold ΔK_{th} for long cracks. For R=0.8 fatigue crack growth rate for short cracks and long cracks is not significantly different and this suggests that crack closure is virtually absent in short cracks.

ACKNOWLEDGEMENTS

This work is financed by the Structures and Materials Panel of AGARD/NATO under the program Additional Support to Portugal (Project P64 - Short Crack Studies

in High Strength Aluminium Alloys).

REFERENCES

(1) - Costa, J.D. and Branco, C.M. "Fracture toughness evaluation of a medium strength Al-Mg alloy", Proc. ECF6, 6th European Conference on Fracture, Netherlands, Ed. EMAS, U.K., 1987, pp.

(2) - Costa, J.D. and Branco, C.M., "Fatigue crack propagation in 5083 Al-alloy", (in portuguese) Proc. Jornadas de Fractura, Lisbon, 1989, Paper Nº. 10.

(3) - Elber, W., "Damage tolerance in aircraft structures" ASTM SPT486, U.S.A., 1971, p.230.

(4) - Ritchie, R.O. and Yu, W. "Short crack effects in fatigue: a consequence of crack tip shielding", "Small fatigue cracks" (Edited by Ritchie, R.O. and Lankford, J.), 1984, pp. 167-189.

(5) - Miller, K.J., "The behaviour of short fatigue cracks and their initiation", FFEMS, Vol. 10, Nº. 2, 1987, pp.75-113.

(6) - Miller, K.J. and Yates, J.R., "Non-propagation fatigue cracks: the true fatigue limit", Proc. NATO ASI Advances in Fatigue Science and Technology, Eds. C. Moura Branco and L. Guerra Rosa, Portugal, Kluwer Academic Publishers, 1989, pp. 253-265.

(7) - Costa, J.D., "Fracture toughness in aluminium alloys", (in portuguese), Msc thesis, University of Coimbra, Department of Mechanical Engineering, Portugal, 1985.

(8) - ASTM E647-87, "Constant load amplitude fatigue crack growth rates above 10^{-8} m/cycle", Annual book of ASTM Standards, U.S.A., 1988.

(9) - Pickard, A.C., "Stress intensity factors with circular and elliptic crack fronts, determined by 3D finite element methods", Proc. 3rd Int. Conf. Numerical Methods in Fracture Mechanics, Ed. Pineridge Press, Swansea, 1984, p.559.

(10) - Newman, J.C. and Raju, J.S., "Stress intensity factor equations for cracks in three dimensional finite bodies subjected to tension and bending loads" NASA TM85793, Virginia, U.S.A., 1984.

(11) - Yoder, G.R., Cooley, L.A., Crooker, T.W., "Fatigue 84", Proc. Int. Conf. on Fatigue and Fatigue Threshold", Edited by C.J. Beevers, EMAS Ltd. Warley, England, 1985, pp. 351-360.

(12) - Pusch, G. and Hohne, V., "Fracture mechanics assessment of an Al-Mg 4.5Mn weld joint", Proc. ECF7, 7th European Conference on Fracture, Budapest, Hungary, published by EMAS, U.K., 1989, pp. 868-871.

(13) - Costa, J.D. and Branco, C.M., "Fatigue behaviour of medium strength Al--Mg alloy 5083", in Advances in Fracture Research, Proc. ICF7, 7th International Conference on Fracture, Houston, Texas, U.S.A., Vol.4, 1990, pp. 2467-2475.

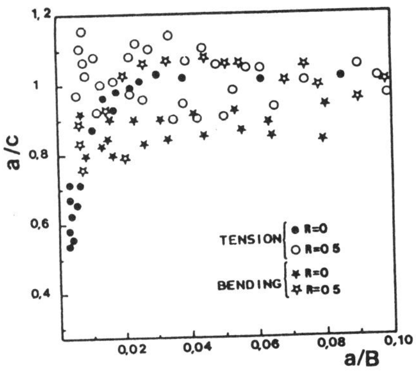

Figure 1 - a/c against a/B. 5083-0 AL alloy. Micro-corner crack.

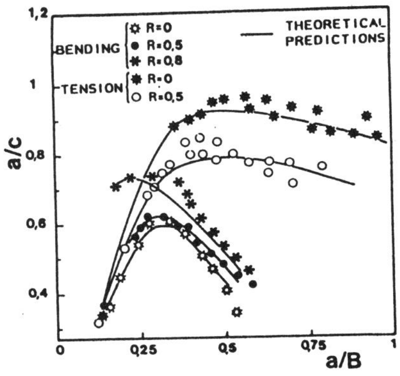

Figure 2 - a/c against a/B. 5083-0 AL alloy. Central semi-elliptical notch.

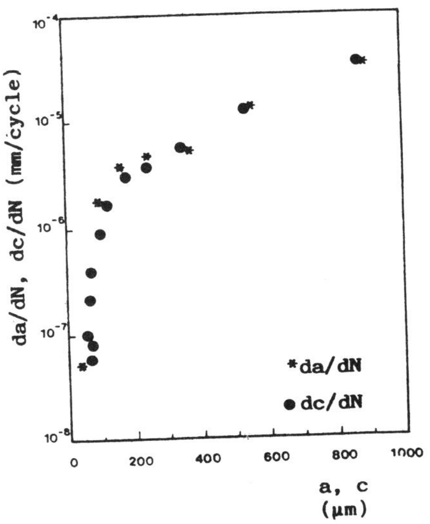

Figure 3 - da/dN against a and dc/dN against c for short cracks. Bending. Al-Mg 5083-0.

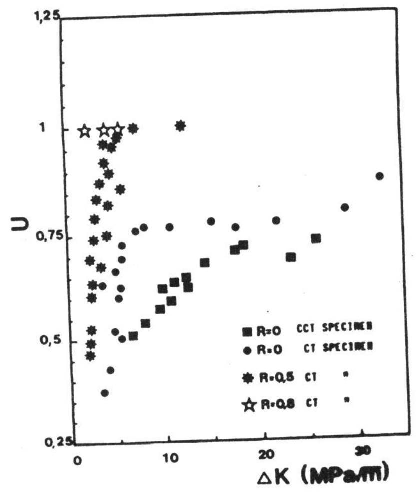

Figure 4 – U against ΔK. Al-Mg alloy 5083-0.

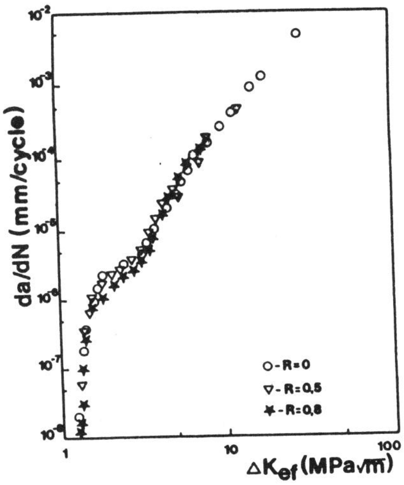

Figure 5 – da/dN against ΔK_{ef}. Al-Mg alloy 5083-0.

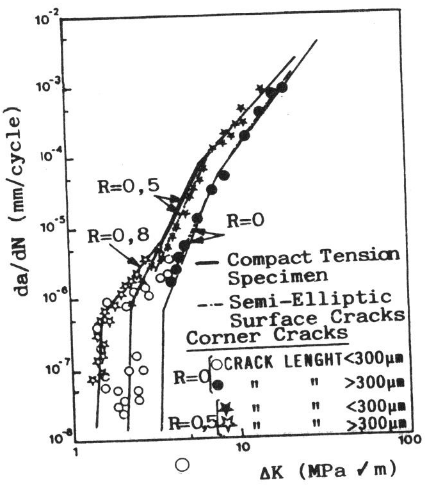

Figure 6 – da/dN against ΔK for short cracks. CT and CCT curves. Al-Mg alloy 5083-0.